Autophagic Protein LC3B Confers Resistance against Hypoxia-induced Pulmonary Hypertension

Seon-Jin Lee[1], Akaya Smith[1], Lanping Guo[2], Tero-Pekka Alastalo[3], Molong Li[3], Hirofumi Sawada[3], Xiaoli Liu[1], Zhi-Hua Chen[1], Emeka Ifedigbo[1], Yang Jin[1], Carol Feghali-Bostwick[2], Stefan W. Ryter[1], Hong Pyo Kim[1,4], Marlene Rabinovitch[3], and Augustine M. K. Choi[1]

[1]Division of Pulmonary and Critical Care Medicine, Brigham and Women's Hospital, Harvard Medical School, Boston, Massachusetts; [2]Division of Pulmonary, Allergy, and Critical Care Medicine, University of Pittsburgh School of Medicine, Pittsburgh, Pennsylvania; [3]Department of Medicine, Stanford University, Stanford, California; and [4]Department of Biological Sciences, College of Natural Sciences, University of Ulsan, Ulsan, Korea

***Rationale*: Pulmonary hypertension (PH) is a progressive disease with unclear etiology. The significance of autophagy in PH remains unknown.**

***Objectives*: To determine the mechanisms by which autophagic proteins regulate tissue responses during PH.**

***Methods*: Lungs from patients with PH, lungs from mice exposed to chronic hypoxia, and human pulmonary vascular cells were examined for autophagy using electron microscopy and Western analysis. Mice deficient in microtubule-associated protein-1 light chain-3B (*LC3B*$^{-/-}$), or early growth response-1 (*Egr-1*$^{-/-}$), were evaluated for vascular morphology and hemodynamics.**

***Measurements and Main Results*: Human PH lungs displayed elevated lipid-conjugated LC3B, and autophagosomes relative to normal lungs. These autophagic markers increased in hypoxic mice, and in human pulmonary vascular cells exposed to hypoxia. Egr-1, which regulates LC3B expression, was elevated in PH, and increased by hypoxia *in vivo* and *in vitro*. *LC3B*$^{-/-}$ or *Egr-1*$^{-/-}$, but not Beclin 1$^{+/-}$, mice displayed exaggerated PH during hypoxia. *In vitro*, LC3B knockdown increased reactive oxygen species production, hypoxia-inducible factor-1α stabilization, and hypoxic cell proliferation. LC3B and Egr-1 localized to caveolae, associated with caveolin-1, and trafficked to the cytosol during hypoxia.**

***Conclusions*: The results demonstrate elevated LC3B in the lungs of humans with PH, and of mice with hypoxic PH. The increased susceptibility of *LC3B*$^{-/-}$ and *Egr-1*$^{-/-}$ mice to hypoxia-induced PH and increased hypoxic proliferation of LC3B knockdown cells suggest adaptive functions of these proteins during hypoxic vascular remodeling. The results suggest that autophagic protein LC3B exerts a protective function during the pathogenesis of PH, through the regulation of hypoxic cell proliferation.**

Keywords: autophagy; hypoxia; hypertension, pulmonary

AT A GLANCE COMMENTARY

Scientific Knowledge on the Subject

Pulmonary hypertension is a progressive disease characterized by increased pulmonary arterial pressure, and subsequent right ventricular failure. The mechanisms of pulmonary vascular remodeling, particularly in the idiopathic form of the disease, remain unclear, but involve endothelial dysfunction and pulmonary vascular cell proliferation.

What This Study Adds to the Field

We have observed the elevated occurrence of autophagy in lung tissue from patients with pulmonary hypertension. This study identifies a role for autophagy as a protective mechanism in lung vascular cells and in the chronic hypoxia mouse model of pulmonary hypertension.

Pulmonary hypertension (PH) is functionally characterized by elevations in mean pulmonary pressure and the development of secondary right ventricular failure. Category I PH, also known as pulmonary arterial hypertension (PAH), includes idiopathic (IPAH), familial, and acquired forms resulting from collagen vascular disease, drugs, HIV infection, portal hypertension, and pulmonary artery shunts (1–5). Categories II–V of PH include those forms secondary to left-heart disease; lung disease or hypoxia; chronic thrombotic or embolic disease; or other diseases rarely associated with PH, such as sarcoid or mediastinitis (1, 2). The molecular and cellular basis for the vascular changes associated with PH remains unclear (6). Impaired production of nitric oxide can result in vasoconstriction and smooth muscle cell proliferation, suggesting a role for endothelial dysfunction in PH (7). In addition, variations in the production, expression, or activity of vascular mediators (i.e., endothelin-1, prostacyclins, voltage-gated K^+-channels), signaling molecules, and growth factors (e.g., transforming growth factor-β, platelet-derived growth factor [PDGF]) have been implicated in hypoxic remodeling seen in PH (8–10). Pulmonary endothelial, smooth muscle, and fibroblast cells, and circulating inflammatory and progenitor cells can all potentially contribute to the remodeling process (10, 11).

Macroautophagy (autophagy) is a cellular homeostatic process involving lysosome-dependent turnover of organelles or proteins (12, 13). Autophagy can be induced in the cardiovascular system by hypoxia, hemodynamic stress, proatherogenic agents, and other noxious stimuli, suggesting a role for this process in vascular adaptation (14, 15). During autophagy, double-membraned autophagic vacuoles or autophagosomes (AV) surround cytosolic organelles (e.g., endoplasmic reticulum, mitochondria) or protein, and subsequently fuse with lysosomes where the engulfed components are enzymatically degraded. By regenerating metabolites (i.e., amino acids, fatty acids) for anabolic pathways, autophagy can prolong survival during starvation (12, 13). Genes critical for the regulation of autophagy (*Atg*) have been identified in mammals, each with distinct roles in the regulation of the autophagic pathway (16). The conversion of microtubule-associated protein-1 light chain 3B (LC3B) from LC3B-I (free form) to LC3B-II (phosphatidylethanolamine

(*Received in original form May 11, 2010; accepted in final form September 30, 2010*)

Supported by NIH grants R01-HL60234, R01-HL55330, R01-HL079904, and P01-HL70807 (A.M.K.C.).

Correspondence and requests for reprints should be addressed to Augustine M.K. Choi, M.D., Pulmonary and Critical Care Medicine, Brigham and Women's Hospital, Harvard Medical School, 75 Francis Street, Boston, MA 02115. E-mail: amchoi@rics.bwh.harvard.edu

This article has an online supplement, which is accessible from this issue's table of contents at www.atsjournals.org

Am J Respir Crit Care Med Vol 183. pp 649–658, 2011
Originally Published in Press as DOI: 10.1164/rccm.201005-0746OC on October 1, 2010
Internet address: www.atsjournals.org

conjugated form) is a major step in autophagosome formation (17, 18).

Autophagy has previously been implicated in human cardiovascular diseases (i.e., heart failure, atherosclerosis, ischemia–reperfusion injury) and other pathologies with either protective or maladaptive roles depending on disease model (14, 15, 19). Here, we have observed enhanced autophagy in clinical samples from patients with several forms of PH. We therefore hypothesized that the autophagic protein LC3B, which is up-regulated in PH tissue and as a response to hypoxia, participates in an adaptive or defense mechanism. To test this hypothesis, we subjected mice genetically deficient in LC3B to chronic hypoxia, and measured indices of PH. We also examined the role of LC3B in the regulation of vascular cell proliferation, a major contributing process to the pathologic phenotype of PH. Our studies suggest that LC3B participates in an adaptive response to hypoxia during the development of PH, as demonstrated by antihypertensive and antiproliferative effects of LC3B. Some of the results of these studies have been previously reported in the form of abstracts (20, 21).

METHODS

An expanded METHODS section is available in the online supplement.

Human Subjects

Lung tissue explants from patients with PH or control subjects were obtained from the University of Pittsburgh Transplant Core Facility. Normal lungs were obtained from patients with traumatic injury unrelated to the lung. For each donor, demographic and clinical data, including echocardiographic and pulmonary arterial pressure data, were obtained (Table 1). Tissue samples (IPAH, n = 5; other forms of PH [non-IPAH], n = 5; or Control, n = 4) were analyzed for autophagic markers by Western immunoblot analysis or for autophagosome formation by electron microscopic analysis as described (*see* online supplement) (22).

TABLE 1. BASELINE CHARACTERISTICS OF PATIENTS*

Pulmonary Hypertension		Control Subjects	
Etiology		Age	36 ± 19
IPAH	5	Sex	
Sarcoid	1	M	2
EtOH	1	F	2
Rheumatic	1		
Congenital	1	Cause of death	Head trauma
Drug induced	1		

	IPAH	Non-IPAH
Age	43 ± 14	48 ± 15
Sex		
M	2	1
F	3	4
Echocardiographic, mm Hg		
RVSP	130 ± 49	95 ± 16
LVEF	>50%	10–50%
Hemodynamic, mm Hg		
PA mean	59 ± 17	49 ± 10
PCWP	7 ± 3	18 ± 5
Six-minute walk, ft	1010 ± 295	1000 ± 95
Therapy		
Flolan	2	2
Remodulin	1	
Flolan, Bosenan	1	1
Flolan, Sildenafil		1
None	1	1

Definition of abbreviations: EtOH = ethanol; IPAH = idiopathic pulmonary arterial hypertension; LVEF = left ventricular ejection fraction; PA = pulmonary arterial; PAP = pulmonary arterial pressure; PCWP = pulmonary capillary wedge pressure; RVSP = right ventricular systolic pressure.

* Lung tissue samples were examined from four normal control subjects and compared with five patients with PAH and five with other forms of PH.

Animals and *In Vivo* Hypoxia Exposure

All animals were housed in accordance with guidelines from the American Association for Laboratory Animal Care. The Animal Research Committee of Brigham and Women's Hospital, Boston, Massachusetts, approved all protocols. Wild-type C57BL/6 mice were exposed to hypoxia 10% O_2 or normoxia for 3 weeks, and then the lungs were harvested and analyzed for autophagic markers by Western analysis or for autophagosome formation by electron microscopic analysis. For functional studies, $LC3B^{-/-}$ mice (8–12 wk old) (23), *Beclin* $1^{+/-}$ mice (24), or early growth response $(Egr\text{-}1)^{-/-}$ mice (Taconic, Germantown, NY) and their corresponding respective age-matched littermates were exposed to 10% O_2 (hypoxia group) or room air (normoxic group) for 4 weeks before functional measurements. For recovery experiments $LC3B^{-/-}$ mice and corresponding $LC3B^{+/+}$ littermates were subjected to 3 weeks of hypoxia followed by 4 weeks of recovery in room air before functional measurements (*see* online supplement).

Vascular Cell Culture

Human pulmonary artery endothelial cells (PAEC) at passages 5–8 were grown to approximately 80% confluence in endothelial cell growth medium-2 (EGM-2) (Lonza; Allendale, NJ). Human pulmonary artery vascular smooth muscle cells (PASMC) at passages 7–10 were grown to approximately 80% confluence in smooth muscle cell growth medium-2 (Lonza). Cells were subjected to transient transfection with either siRNA or expression vectors to modulate the cellular expression of LC3B or Egr-1. For proliferation experiments, transiently transfected cells at 80% confluence were starved for 2 hours in serum-free EGM-2 media before the addition of PDGF-BB (20 ng ml^{-1}) or endothelin-1 (40 nM) in complete growth media, and then placed in hypoxia or normoxia for an additional 48 hours. For hypoxic exposures, PAEC or PASMC were incubated in an atmosphere of 1% O_2, 5% CO_2, and 94% N_2 for the indicated intervals. Corresponding normoxic controls were maintained for equivalent times in humidified incubators in an atmosphere of 95% air and 5% CO_2. Cell proliferation was assessed for proliferation using a standard MTT assay and cell counting, or for the expression of specific proteins by Western analysis (*see* online supplement).

Statistics

Data are presented as mean ± SD. Paired analysis was performed with the Student *t* test as appropriate. Parametric analyses were performed by one-way analysis of variance with Tukey method. Correlations between parameters were expressed with the Pearson correlation coefficient (*r*). Statistical significance was accepted at $^{*}P$ less than 0.05 and $^{\#}P$ less than 0.01 (Figures 1 and 3–7).

RESULTS

Increased Autophagy in PAH

Lung tissue sections from normal patients and patients with PH (Table 1) were analyzed for the expression of LC3B. In human lung tissue derived from patients with strictly IPAH, the total expression of LC3B and the relative expression of its activated (lipidated) form LC3B-II (Figure 1A, *upper panel*) were markedly increased relative to normal lung tissue. Similar results were obtained from samples with other forms of PH (Table 1 and Figure 1A, *lower panel*). The changes in LC3B expression corresponded to increased *LC3B* mRNA in human PH lung (Figure 1B). Immunohistochemical staining of pulmonary vascular tissue from normal or PH lung revealed the increased expression of autophagic markers in PH tissue relative to normal tissue. The expression of LC3B was markedly increased in the endothelial cell layer, and in the adventitial and medial regions of large and small pulmonary resistance vessels from PH lung, relative to normal vascular tissue (Figure 1C).

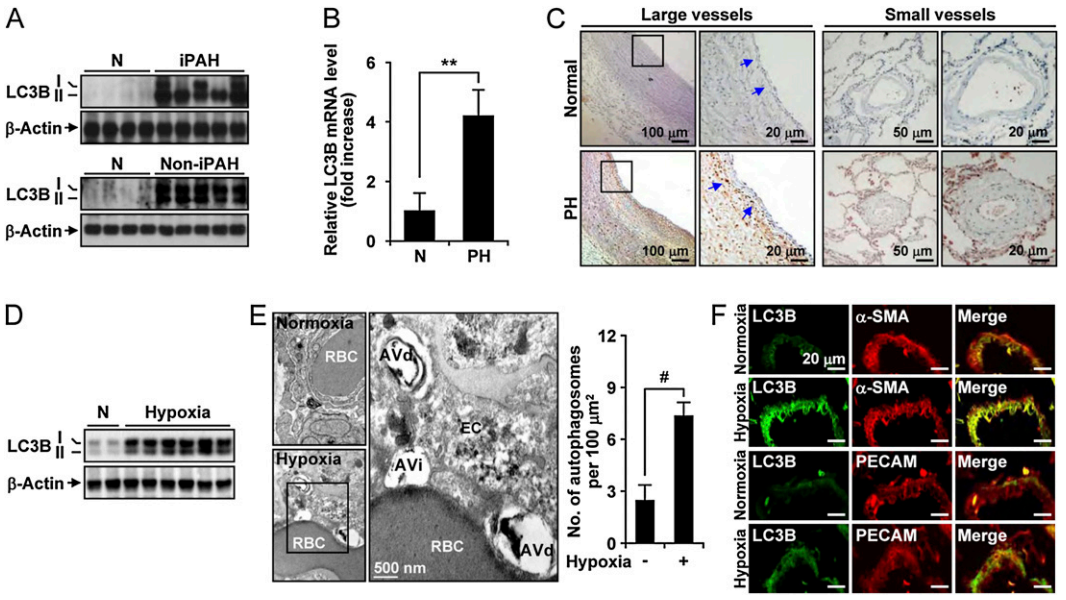

Figure 1. Autophagy is increased in the lung and lung vasculature of patients with human pulmonary hypertension (PH), and in the lung and lung vascular tissue of mice exposed to chronic hypoxia. (*A*) Western blot analysis of light chain-3B (LC3B)-I/-II expression in lung tissue from normal patients (N) and patients with idiopathic pulmonary arterial hypertension (IPAH) or non-IPAH forms of PH (*see* Table 1 for demographics). β-actin served as the standard (n = 4 normal, n = 5 PAH, and n = 5 patients with PH). (*B*) The level of LC3B mRNA from normal (n = 5) and patients with PH (n = 10) was measured by reverse transcriptase polymerase chain reaction. 18S rRNA served as the standard. Data are mean ± SD. $^{**}P < 0.0001$. (*C*) Immunohistochemical analysis of LC3B protein in large (*left*) and small (*right*) human pulmonary vessels from normal or PH lung. *Blue arrows* indicate staining in the vessel intima and adventitia. Scale bars represent 10–100 μm as indicated. (*D*) Expression of LC3B in lung tissues from mice exposed to chronic hypoxia (10% O_2, 3 wk) or normoxia (N). Total LC3B expression was normalized to β-actin. (*E*) Representative electron micrograph of mouse lung tissue from chronic hypoxia–treated mice and corresponding normoxic controls. Immature autophagic vacuoles (AVi) and degradative autophagic vacuoles (AVd) are detected in an endothelial cell (EC). AV were scored as described elsewhere (22). A red blood cell (RBC) is observed within the vessel lumen. Scale bar represents 500 nm. Total AV formation per 100 μm^2 is quantitated at right. Data represent mean ± SD. n = 15 electron microscope images per condition, $^{\#}P < 0.01$. (*F*) The expression of LC3B is localized in EC and smooth muscle actin (SMA) in mice lung tissue. Sections of vessels isolated from hypoxia-treated mice were stained for LC3B (rabbit antimouse) using fluorescein isothiocyanate–conjugated secondary antibodies, or stained for α-SMA or platelet endothelial cell adhesion molecule-1 (PECAM) (rat antimouse) as indicated, using Cy3-conjugated IgG secondary antibodies. LC3B localized to the vessel wall. Merged images demonstrate colocalization to the endothelial and smooth muscle cells as indicated by α-SMA and PECAM antibodies. All panels are at ×40 magnification. *Scale bars* = 20 μm.

To determine the role of autophagy in PH, we examined this process in a mouse model of hypoxia-induced PH. In mice, 3 weeks of hypoxia (10% O_2), which induces PH in these animals, increased total LC3B expression and LC3B-II accumulation in lung tissue (Figure 1D). Electron microscopic analysis revealed that immature (AVi) and degradative (AVd) AV (22) were dramatically increased in hypoxic lung tissues, relative to lung tissue from air-treated controls (Figure 1E). Quantification of

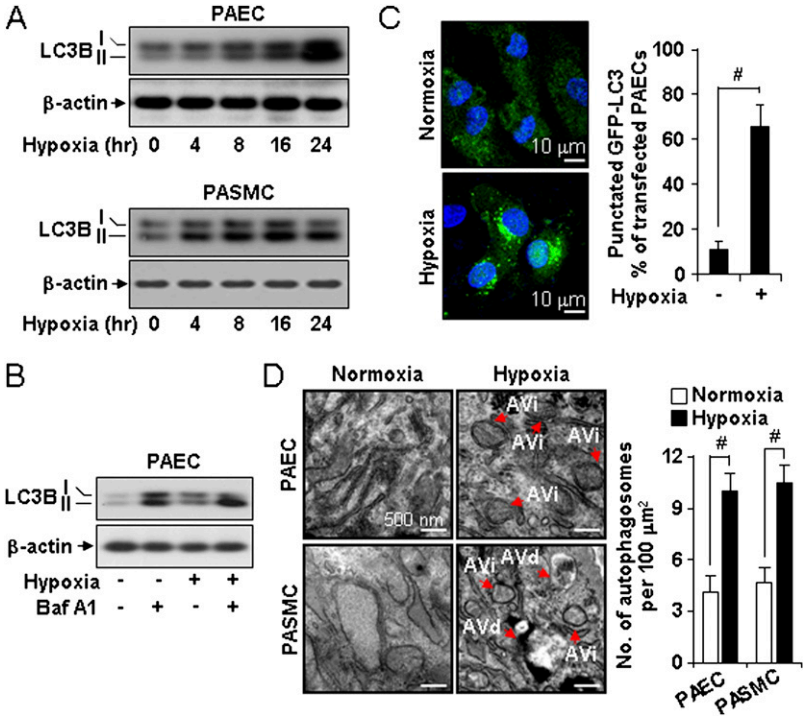

Figure 2. Hypoxia increased the expression and activation of light chain-3B (LC3B) in pulmonary vascular cells *in vitro*. (*A*) pulmonary artery endothelial cells (PAEC) and pulmonary artery vascular smooth muscle cells (PASMC) were exposed to hypoxia for 0–24 hours and evaluated for expression of LC3B-I and LC3B-II by Western analysis. β-actin served as the standard. (*B*) PAEC were exposed to hypoxia for 24 hours in the absence or presence of bafilomycin A1 (100 nM), and evaluated for the expression of LC3B-I and LC3B-II by Western analysis. β-actin served as the standard. (C) PAEC transfected with green fluorescence protein–LC3 were exposed to hypoxia or normoxia for 24 hours. Cells were visualized by confocal microscopy and the percentage of cells exhibiting punctuated green fluorescence protein–LC3 fluorescence was calculated relative to all green fluorescence protein–positive cells. Data represent mean ± SD. $^{\#}P < 0.01$. (*D*) Electron microscopic analysis of PAEC and PASMC after 24 hours of hypoxia. *Red arrows* indicate the presence of immature (AVi) or degradative (AVd) autophagic vacuoles. AV were scored as described in reference (22). Scale bar = 500 nm. Graphs represent quantification of autophagosomes (AVi + AVd) per cell in PAEC and PASMC exposed to hypoxia or normoxia. Data represent mean ± SD. n = 15 electron microscope images per cell type and condition, $^{\#}P < 0.01$.

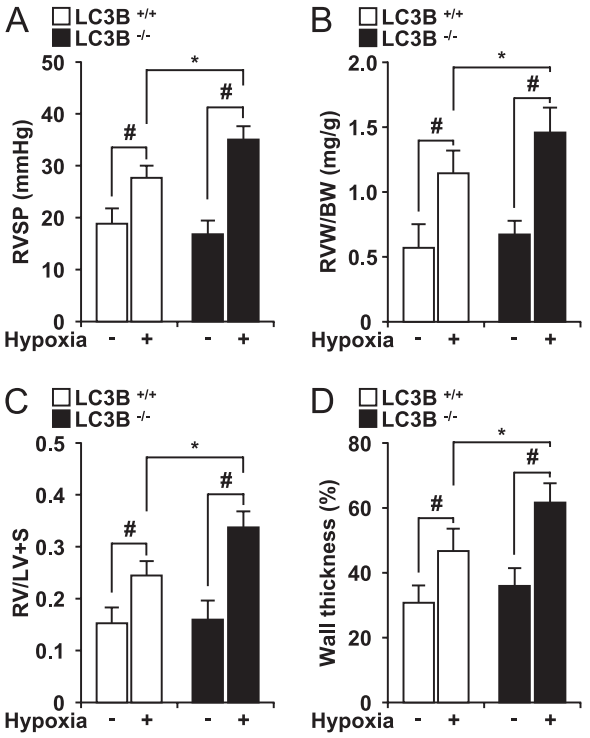

Figure 3. Light chain-3B (*LC3B*$^{-/-}$) mice display enhanced indices of pulmonary hypertension after chronic hypoxia. (*A*) Right ventricular systolic pressure (RVSP) was measured in *LC3B*$^{+/+}$ (*open square*) and *LC3B*$^{-/-}$ (*black square*) mice after hypoxia (n = 15) and normoxia (n = 15) for 4 weeks. (*B*) Right ventricle weight (RVW) (milligrams) normalized for body weight (BW) (grams) in *LC3B*$^{+/+}$ (*open square*) and *LC3B*$^{-/-}$ (*black square*) mice. (*C*) Fulton index of right ventricular hypertrophy (RVH), measured as ratio of the RVW to that of the left ventricle plus septum (RV/LV+S). (*A*–*C*) Data represent mean ± SD (n = 5). $^{\#}P < 0.01$; $^{*}P < 0.05$. (*D*) Graphic shows quantitation of percent wall thickness of pulmonary arterioles in the lungs of *LC3B*$^{+/+}$ (*open square*) and *LC3B*$^{-/-}$ (*black square*) mice after normoxia (n = 10 per group) and hypoxia (n = 10 per group). Data are expressed as mean ± SE ($^{*}P < 0.05$; $^{\#}P < 0.01$) for hypoxic *LC3B*$^{-/-}$ mice versus hypoxic *LC3B*$^{+/+}$ mice and corresponding normoxic controls.

electron micrographs (n = 15) revealed that total AV were significantly increased in hypoxic lung tissue (Figure 1E). The expression of LC3B in small pulmonary vessels from hypoxia-treated animals was evaluated using confocal microscopy (Figure 1F). The expression of LC3B in lung vascular tissue was induced by hypoxia, and colocalized with markers of smooth muscle and endothelial cells as shown in the merged images.

Hypoxia Increases Autophagy in Primary Pulmonary Vascular Cells *In Vitro*

We examined the expression of autophagic markers in primary human pulmonary vascular cells including human PAEC and PASMC during hypoxia exposure (1% O_2) *in vitro*. Hypoxia exposure induced time-dependent increases of LC3B expression and the accumulation of its active form (LC3B-II) in PAEC (Figure 2A, *upper panel*). Similar results of LC3B activation were observed in PASMC (Figure 2A, *lower panel*). To determine whether increases in LC3B activation correlated with increased autophagic flux during hypoxia treatment, we repeated these experiments in the absence or presence of bafilomycin-A1, an inhibitor of autophagosome-lysosome fusion (25). Bafilomycin-A1 treatment further elevated the expression of LC3B-II in PAEC under both normoxic and hypoxic exposures, indicative of autophagic activity under these conditions (Figure 2B). We also examined the response in primary mouse lung microvascular endothelial cells. Similar results were obtained with respect to activation of LC3B-II and enhancement of the response by bafilomycin-A1 (*see* Figures E1A and E1B).

We examined morphologic indices of autophagy in hypoxia-treated pulmonary vascular cells. Hypoxia treatment (1% O_2, 24 h) of green fluorescence protein–LC3-transfected PAEC induced the formation of green fluorescence protein-LC3 puncta, an indicator of autophagosome formation (Figure 2C) (25, 26). Hypoxia treatment resulted in increased formation of AVi and AVd after 24 hours exposure in PAEC and PASMC (Figure 2D).

LC3B$^{-/-}$ Mice Display Enhanced Indices of PH in the Chronic Hypoxia Model

We sought to examine the functional role of LC3B during the development of PH. To test the hypothesis that *LC3B*$^{-/-}$ mice (23) are more susceptible to PH, we measured right ventricular systolic pressure (RVSP) in *LC3B*$^{-/-}$ or *LC3B*$^{+/+}$ littermate mice subjected to hypoxia (10% O_2). Under normoxic conditions, *LC3B*$^{-/-}$ mice displayed similar RVSP relative to *LC3B*$^{+/+}$ mice (Figure 3A). In *LC3B*$^{-/-}$ mice (n = 15), 4-week hypoxia exposure increased RVSP approximately two-fold relative to baseline, and this value was significantly higher than that of hypoxia-exposed *LC3B*$^{+/+}$ mice (n = 15). Right ventricular hypertrophy, as measured by the ratio of right ventricle weight to body weight (RVW/BW) or by the ratio of RVW to combined left ventricle and septum weight (RV/LV+S) (Fulton index), was significantly greater in *LC3B*$^{-/-}$ mice (n = 15) than in *LC3B*$^{+/+}$ mice (n = 15) after 4 weeks of hypoxia (Figures 3B and 3C). Both *LC3B*$^{-/-}$ and *LC3B*$^{+/+}$ mice displayed comparable RVW/BW and RV/LV+S under normoxia (Figures 3B and 3C). Hematoxylin and eosin staining revealed enhanced vascular remodeling in *LC3B*$^{-/-}$ mice after hypoxia compared with *LC3B*$^{+/+}$ mice (Figure E2A). *LC3B*$^{-/-}$ mice developed exaggerated vascular remodeling with a significant increase in wall thickness of pulmonary arterioles (61 ± 7.4%) after hypoxia compared with *LC3B*$^{+/+}$ mice (43.7 ± 5.6%; $P < 0.05$) and respective normoxic controls (Figures 3D and E2A). Consistent with these findings, α-smooth muscle actin (α-SMA) expression was increased in lung tissue by chronic hypoxia, indicative of active remodeling processes. The α-SMA expression was considerably enhanced in *LC3B*$^{-/-}$ mice relative to *LC3B*$^{+/+}$ mice, in response to hypoxia (Figure E2B). The phenotypes of *LC3B*$^{-/-}$ and *LC3B*$^{+/+}$ mice with respect to lung LC3B expression were validated (Figure E2B). To further assess the role of LC3B in susceptibility to hypertension, *LC3B*$^{-/-}$ or *LC3B*$^{+/+}$ littermate mice were subjected to hypoxia for 3 weeks and then allowed to recover in room air for 4 weeks. At the end of the recovery period, *LC3B*$^{-/-}$ mice displayed significantly greater elevation of RVSP (n = 6 per group) (Figure E3A) and RV/LV+S (n = 8 per group) (Figure E3B), relative to *LC3B*$^{+/+}$ mice.

To further evaluate the prospective role of autophagy in these observations, similar analyses were performed using mice with heterozygous disruption of another major autophagic regulator protein, Beclin 1. *Beclin 1*$^{+/-}$ mice or *Beclin 1*$^{+/+}$ littermate mice were subjected to hypoxia (10% O_2) for 4 weeks. No significant changes in the vascular response were noted in *Beclin 1*$^{+/-}$ mice relative to *Beclin 1*$^{+/+}$ mice with respect to RSVP and RV/LV+S measurements (Figure E4). We also evaluated the effect of the autophagic inhibitor chloroquine on the development of PH in wild-type mice. Chloroquine injection did not change the vascular response in mice subjected to hypoxia or in rats treated with monocrotaline, an alternative model of PH development (Figure E5).

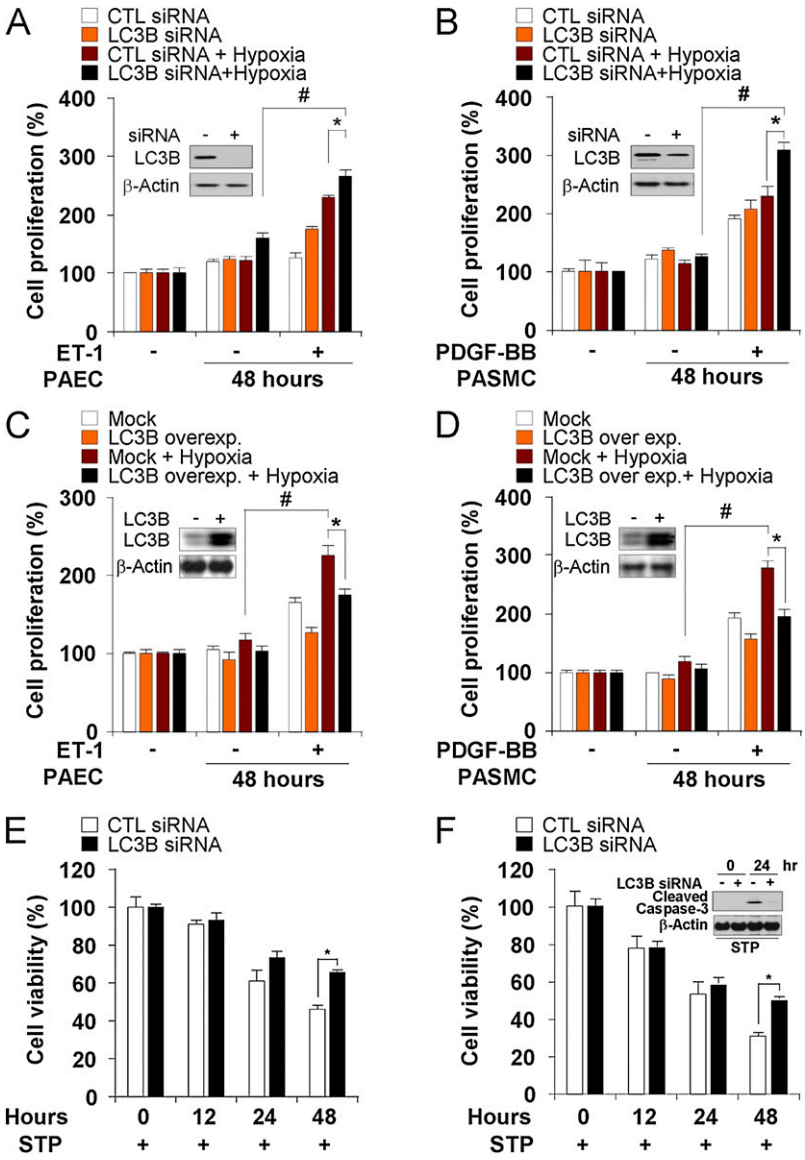

Figure 4. Light chain-3B (LC3B) modulates pulmonary vascular cell proliferation. (*A* and *B*) Pulmonary artery endothelial cells (PAEC) and pulmonary artery vascular smooth muscle cells (PASMC) were transfected with control or *LC3B* siRNA then endothelin (ET)-1 (40 nM) or platelet-derived growth factor (PDGF)-BB (20 ng ml^{-1}) were added to PAEC (*A*) and PASMC (*B*) for 48 hours, respectively. Cultures were then exposed to hypoxia or normoxia for an additional 48 hours. Proliferation was assessed by MTT assay. Data represent mean ± SD (n = 3). $^{*}P < 0.05$; $^{\#}P < 0.01$. (*C* and *D*) PAEC and PASMC were transfected with control or pCMV-LC3 expression vector and then ET-1 (40 nM) or PDGF-BB (20 ng ml^{-1}) were added to PAEC (*C*) and PASMC (*D*) for 48 hours, respectively. Cells were exposed to hypoxia or normoxia for an additional 48 hours. Proliferation was assessed by MTT assay. Data represent mean ± SD (n = 3). $^{*}P < 0.05$; $^{\#}P < 0.01$. (*A–D*) Western analysis was used to validate targeted changes in LC3B expression in PAEC and PASMC with β-actin as the standard (*inserts*). (*E* and *F*) LC3B modulates pulmonary vascular cell apoptosis (*E*) PAEC and (*F*) PASMC were transfected with control or *LC3B* siRNA and then exposed to hypoxia or normoxia for 0–48 hours in the presence of staurosporine (1 μM). Cell death was assessed by crystal violet staining. Data represent mean ± SD (n = 3). $^{*}P < 0.05$. Western blot analysis was used to assay caspase-3 cleavage in PASMC with β-actin as the standard (*insert*).

Role of LC3B in Vascular Cell Proliferation

We next evaluated the role of LC3B in pulmonary vascular cell proliferation *in vitro*. Stimulation with endothelin-1 (40 nM) or PDGF-BB (20 ng · ml^{-1}) for 48 hours during hypoxia increased cell proliferation in PAEC (Figure 4A) and PASMC (Figure 4B), respectively. Infection with *LC3B*-specific siRNA further increased hypoxia and mitogen-dependent cell proliferation relative to control siRNA-infected cells. Conversely, overexpression of LC3B by transfection with LC3B expression vector decreased hypoxia and mitogen-dependent cell proliferation in PAEC (Figure 4C) and PASMC (Figure 4D), relative to control transfected cells. Interestingly, the *LC3B*-specific siRNA-infected PAEC (Figure 4E) and PASMC (Figure 4F) also displayed attenuated activation of staurosporine-induced apoptosis (caspase-3 cleavage) compared with control siRNA-infected cells.

LC3B Suppresses Reactant Oxygen Species–Dependent Stabilization of Hypoxia-inducible Factor-1α

We next evaluated the potential role of the hypoxia-inducible factor (HIF)-1α pathway, a major regulatory of proliferative responses to hypoxia, in the antiproliferative effects of LC3B. Increases in cellular reactive oxygen species (ROS) production are known to promote HIF-1α stabilization (27). PAEC cells infected with LC3B-specific siRNA displayed a greater accumulation of intracellular ROS production under both normoxic and hypoxic conditions, relative to control siRNA-transfected cells (Figures 5A and 5B). Similarly, LC3B knockdown cells displayed greater HIF-1α levels under normoxic and hypoxic conditions (Figure 5C).

Egr-1 Regulates LC3B during Hypoxia *In Vitro* and *In Vivo*

Genetic analysis of the promoter region of *LC3B* revealed consensus binding sites for the Egr-1 transcription factor (28). We hypothesized that Egr-1 regulates *LC3B* expression and autophagy during hypoxia. Chromatin immunoprecipitation assays revealed that Egr-1 was rapidly induced to bind the *LC3B* promoter after stimulation by hypoxia in PAEC (Figure 6A). Human PH lung tissue displayed increased Egr-1 protein expression relative to normal lung tissue (n = 5 normal, n = 10 PH) (Figure 6B). Egr-1 protein expression was also increased in mouse lung tissue after 4 weeks hypoxia treatment (n = 3 per each group) (Figure 6C).

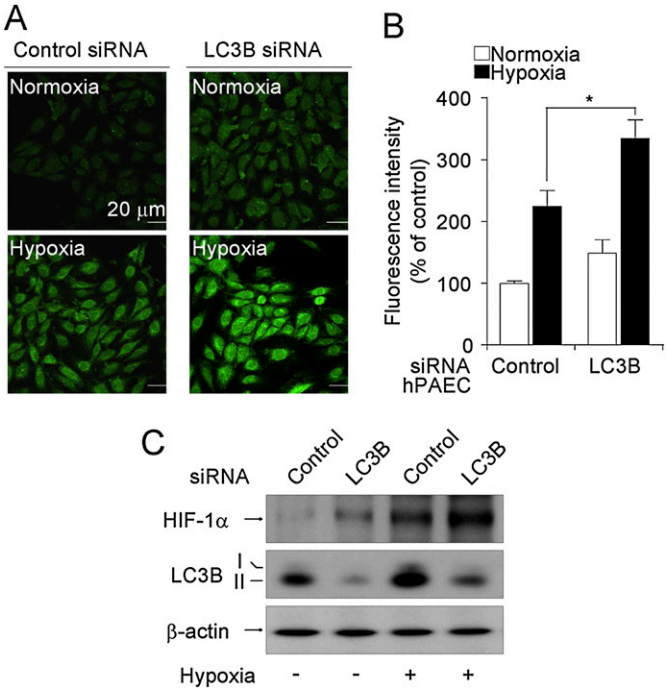

Figure 5. Light chain-3B (LC3B) knockdown increases intracellular reactive oxygen species production and stabilizes hypoxia-inducible factor (HIF)-1α. Pulmonary artery endothelial cells (PAEC) were infected with LC3B-siRNA or control siRNA. Infected PAECs were treated with hypoxia (1%) exposure for 30 minutes and incubated with 10 μM H_2DCF-DA for another 30 minutes at 37°C. After the excess probe was removed, cells were incubated for an additional 20 minutes before fluorescence confocal microscopy. (*A*) Representative fluorescence images are shown. (*B*) The relative fluorescence in the treatment groups is quantitated (n = 10). *$P < 0.5$. (*C*) Cell lysates were analyzed for HIF-1α stabilization by Western immunoblot analysis. β-actin was used as the standard.

We investigated the influence of Egr-1 expression on LC3B protein levels in hypoxia-treated cells. Infection of PAEC with *Egr-1*–specific siRNA inhibited the expression of LC3B during 24 hours continuous hypoxia (Figure 6D).

Egr-$1^{-/-}$ Mice Display Reduced Autophagy and Enhanced Indices of PH during Hypoxia

To obtain evidence for the involvement of Egr-1 expression in hypoxia-induced autophagy *in vivo*, we examined LC3B expression in *Egr-*$1^{+/+}$ or *Egr-*$1^{-/-}$ mice (n = 3). Exposure of *Egr-*$1^{+/+}$ mice to hypoxia caused significant increases in LC3B in the lung. However, LC3B expression was not detectable in *Egr-*$1^{-/-}$ lung tissue (Figure 7A). We hypothesized that *Egr-*$1^{-/-}$ mice may be susceptible to hypoxia-induced PH. We measured RSVP in *Egr-*$1^{-/-}$ mice and *Egr-*$1^{+/+}$ littermate mice subjected to chronic hypoxia. *Egr-*$1^{-/-}$ mice and *Egr-*$1^{+/+}$ mice displayed comparable RVSP in normoxia (Figure 7B). In *Egr-*$1^{-/-}$ mice (n = 3), 4-week hypoxia exposure (10% O_2) increased RSVP compared with baseline, and this value was markedly higher than RSVP in hypoxic *Egr-*$1^{+/+}$ mice (n = 3) (Figure 7B). Right ventricular hypertrophy, as measured by RVW/BW and RV/LV+S, was also greater in hypoxia-exposed *Egr-*$1^{-/-}$ mice, relative to *Egr-*$1^{+/+}$ mice (Figures 7C and 7D).

Histologic analysis revealed increased pulmonary vascular remodeling in *Egr-*$1^{-/-}$ mice exposed to chronic hypoxia, as evidenced by α-SMA staining (Figure E6). Analysis of autophagic activation (colocalization of LAMP-1 and LC3B) revealed impaired autophagy in response to hypoxia in cultured lung fibroblasts from *Egr-*$1^{-/-}$ mice relative to *Egr-*$1^{+/+}$ pulmonary fibroblasts (Figure E7).

LC3B and Egr-1 Localize to Caveolae and Interact with Caveolin-1

We isolated caveolae fractions from PAEC subjected to normoxia or hypoxia *in vitro*. Caveolin-1, which is constitutively expressed in caveolae (29), localized in fractions (3–5) (Figure E8A). Lipid raft isolation was confirmed using GM-1, an independent marker of plasma membrane lipid rafts, which also localized to fractions (3–5). LC3B localized to the GM1- and caveolin-1–containing fractions under normoxia in PAEC and PASMC (Figure 8A). However, hypoxia diminished LC3B abundance in the caveolae in PAEC and PASMC (Figure 8A). Similarly, we observed the caveolae localization of Egr-1 in PAEC and PASMC under normoxia, and the loss of Egr-1 from caveolae under hypoxia (Figure 7A). We further evaluated the localization of caveolin-1 and LC3B in PAEC under normoxia and hypoxia using confocal microscopy. Caveolin-1 and LC3B

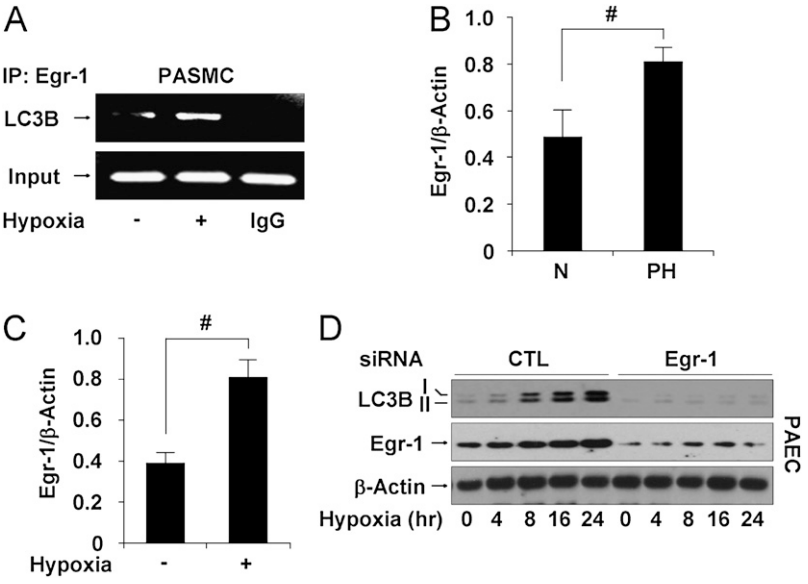

Figure 6. Early growth response (Egr)-1 regulates hypoxia-induced light chain-3B (LC3B) expression *in vitro* and *in vivo*, and protects against pulmonary hypertension during chronic hypoxia. (*A*) Pulmonary artery vascular smooth muscle cells (PASMC) were treated with hypoxia (1% O_2) for 8 hours. Chromatin samples were immunoprecipitated with anti–Egr-1 and evaluated for factor binding to the *LC3B* promoter region. (*B*) Egr-1 expression relative to β-actin was evaluated in lung homogenate from normal patients (N) and patients with pulmonary hypertension (PH) by quantification of Western blots. Data represent mean ± SD (n = 5 normal, n = 10 PH). #$P < 0.01$. (*C*) The protein levels of Egr-1 in mouse lung tissues harvested from animals exposed to hypoxia and normoxia were evaluated by Western analysis. Data represent mean ± SD (n = 6). #$P < 0.01$. (*D*) Pulmonary artery endothelial cells (PAEC) were infected with Egr-1–specific siRNA or control siRNA, then treated with hypoxia (1% O_2) for 0–24 hours. Expression of LC3B and Egr-1 was determined by immunoblotting with β-actin as the standard.

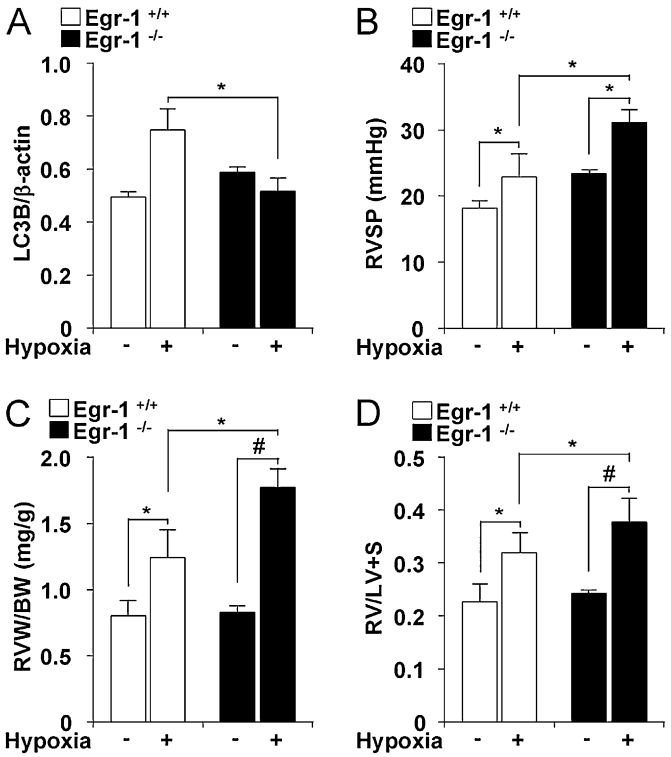

Figure 7. Early growth response (Egr-1)$^{-/-}$ mice display enhanced indices of pulmonary hypertension after chronic hypoxia. (*A*) *Egr-1*$^{+/+}$ and *Egr-1*$^{-/-}$ were exposed to chronic hypoxia. Lung tissue was analyzed for light chain-3B (LC3B) by Western blotting. β-actin served as the standard. *$P < 0.05$; $^{\#}P < 0.01$. (*B*) Right ventricular systolic pressure (RVSP) was measured in *Egr-1*$^{+/+}$ (*open square*) and *Egr-1*$^{-/-}$ (*black square*) mice after exposure to hypoxia and normoxia for 4 weeks. Data represent mean ± SD (n = 3). (*C*) Right ventricular weight (RVW, milligrams) normalized for body weight (BW, grams) in *Egr-1*$^{+/+}$ (*open square*) and *Egr-1*$^{-/-}$ (*black square*) mice. (*D*) Fulton index of right ventricle hypertrophy measured as ratio of the weight of the RV to that of the left ventricle (LV) plus septum (RV/LV+S). (*C* and *D*) Data represent mean ± SD (n = 3) *$P < 0.05$; $^{\#}P < 0.01$.

localized to the plasma membrane, with diffuse cytoplasmic staining under normoxia (Figure E8B). Hypoxia induced the translocation of both caveolin-1 and LC3B from the membrane to the cytoplasm in PAEC by 24 hours (Figure E8B). Importantly, hypoxia exposure did not affect the abundance or distribution of GM1, confirming the specificity of the response (Figure E8A). To examine if caveolin-1 is involved in hypoxia-induced autophagy and trafficking of LC3B, PAEC were exposed with hypoxia for 8 hours and caveolae fractions (Figures 8B and 8C) were isolated. In normoxic PAEC, an interaction between LC3B and caveolin-1 was detected in caveolae fractions by coimmunoprecipitation, indicating the localization of LC3B to caveolae in association with caveolin-1. Treatment of these cells with hypoxia caused the time-dependent disruption of this complex (Figure 8B). An interaction of Egr-1 with caveolin-1 was also detected in caveolae fractions from PAEC under normoxia, with time-dependent dissociation of this complex under hypoxia (Figure 8C). Similar results were observed in PASMC (Figures 8D and 8E).

DISCUSSION

We demonstrate here for the first time the elevated occurrence of autophagy, as exemplified by increases in morphologic and biochemical markers of this process, in human clinical samples from patients with PH. Although autophagy has been investigated in several preclinical models of human disease (19), including cancer (30, 31), neurodegenerative diseases (32), heart disease (15), inflammatory bowel disease (33), and chronic lung disease (28), few studies have examined this process in human tissue samples.

The regulation and function of autophagy in human disease is currently not well understood. Because of its basic role in lysosomal degradation and recycling of metabolic precursors, autophagy is generally considered a cell survival pathway (12, 13). However, excessive activation of autophagy has also been associated with cell death (i.e., caspase-independent or autophagic cell death) (34, 35).

In the current study, we have also demonstrated increased autophagy in the lung vasculature of mice in the chronic hypoxia mouse model of PH, and in cultured human pulmonary vascular cells exposed to hypoxia. We have shown that chronic hypoxia, in the context of an animal model of hypoxia-induced PH, induces autophagosome formation, and the synthesis and activation of LC3B in mouse lung vascular tissue. These initial observations demonstrate activation of LC3B and implicate the process of autophagy as a general response to hypoxic stress in the pulmonary vasculature. Furthermore, in addition to the studies shown in the current article using the hypoxia model of PH, we have observed activation of the major autophagic protein LC3B in three additional animal models of PH. LC3B activation was observed in rat lungs 3 weeks after a single injection of monocrotaline (60 mg/kg subcutaneously), an established model of rat PH relative to vehicle controls (Smith and Choi unpublished data). In two independent mouse models that develop spontaneous PH, including transgenic mice overexpressing IL-6 Tg (36) and mice genetically deleted for vasoactive intestinal peptide (37) (Lee, Smith, and Choi, unpublished data), we also have observed elevated activation of LC3B in the lungs of mice from both of these models. Detailed characterization of these additional models of PH is beyond the scope of the current manuscript, but will be the focus of future studies. The combined observations of the elevated occurrence of autophagy in human tissue with PH of various etiologies including PAH, and the elevated occurrence of autophagy in several animal models of stress-induced or genetically induced PH, lend credence to the proposed hypothesis that autophagic proteins, such as LC3B, could have important functional roles in the development or progression of PH.

The elevated occurrence of autophagy in patients with severe PH could suggest an insufficient repair response. However, our functional experiments using the mouse model of hypoxia-induced PH demonstrated that a major autophagic protein, LC3B, can play a role in limiting the progression of PH.

Our results in animal models indicate a protective role for LC3B in responses of the pulmonary circulation to hypoxia. This conclusion arises from observations of aggravated indices of PH (i.e., RSVP, Fulton index); increased vascular wall thickness; and enhanced α-SMA expression in animals genetically deleted for the autophagic regulator protein LC3B in the chronic hypoxia model. Furthermore, knockdown of LC3B enhanced the proliferation of hypoxic PAEC and PASMC. Conversely, overexpression of LC3B inhibited the hypoxic proliferation of these vascular cell lines. These experiments suggest that active LC3B in vascular cells may partially inhibit the proliferative processes that drive hypoxic remodeling.

A similar paradigm for autophagic protein activation as a protective but insufficient response to stress has recently been shown in the work of Nakai and coworkers (38). In this study an increase in the expression of the autophagic protein Atg5 was demonstrated in the failing mouse heart after severe hemodynamic stress when compared with the nondiseased state. However, cardiac-specific deficiency in the autophagic regulator protein Atg5 resulted in more rapid development of heart failure under

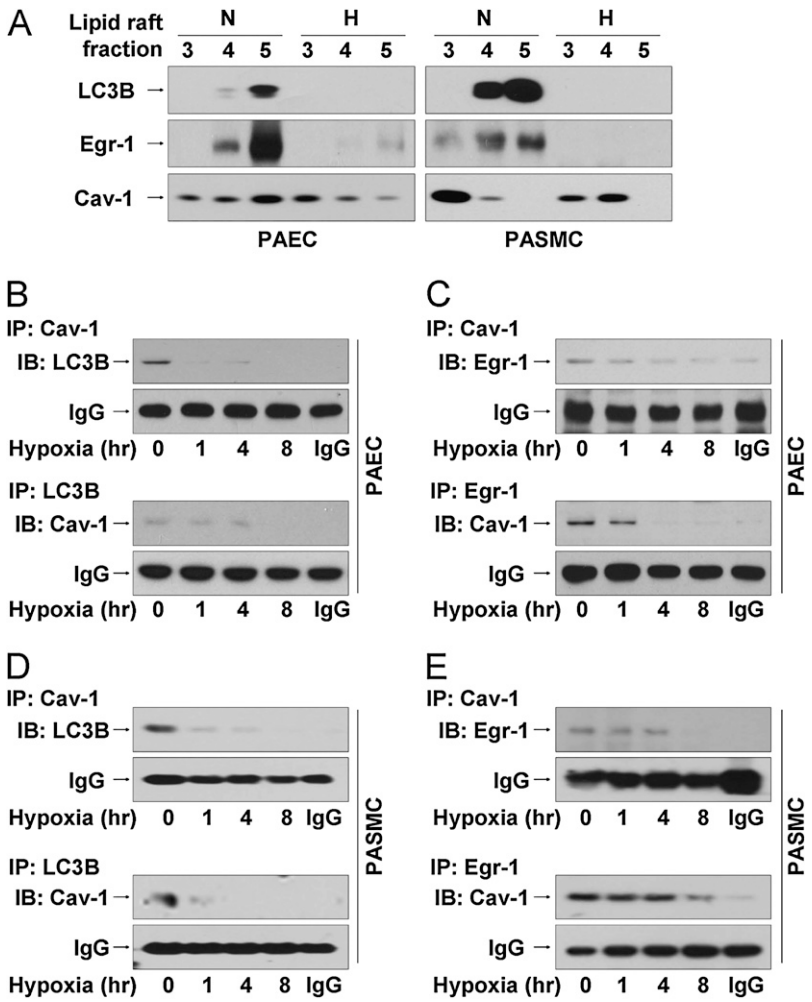

Figure 8. Light chain-3B (LC3B) and early growth response (Egr)-1 localize to the lipid rafts and form complexes with caveolin (Cav)-1, which are displaced by hypoxia. (*A*) Human pulmonary artery endothelial cells (PAEC) and pulmonary artery vascular smooth muscle cells (PASMC) were exposed to hypoxia or normoxia for 24 hours. Cell lysates were subjected to sucrose density gradient ultracentrifugation, to isolate 12 fractions (*see* Figure E5A). Fractions (3–5) corresponding to lipid rafts were immunoblotted for Egr-1, LC3B, or Cav-1. PAEC (*B* and *C*) or PASMC (*D* and *E*) were exposed to hypoxia for 0–8 hours. Cell lysates were subjected to sucrose density gradient fractionation. Fractions (3–5) were subjected to immunoprecipitation with anti–Cav-1 followed by immunoblotting with anti-LC3B (*B* and *D*) or anti–Egr-1 (*C* and *E*). Reciprocal co-IP was performed for each experiment. IgG served as the standard.

hemodynamic stress, suggesting a cardioprotective role (38). Increased autophagy has also been observed as a general stress response to nutrient starvation. Mice genetically deleted in Atg5 (*Atg5*$^{-/-}$), which display impaired autophagy in response to starvation, were more susceptible to cardiac dysfunction after starvation (39). Elevated autophagy was also detected as a stress response during cardiac ischemia–reperfusion injury in the mouse. In this model Beclin 1 hemizygous mice displayed reduced autophagy during ischemia–reperfusion and were resistant to ischemia–reperfusion induced cardiac injury (40). Thus, autophagic proteins have been implicated in both protective and maladaptive roles depending on the stress model.

Previously, enhanced tumorigenesis in *Beclin 1*$^{+/-}$ mice has been attributed to genomic instability resulting from increased metabolic stress and impaired autophagy (41). In our current studies, however, the functional differences in the hypoxic response of the lung vasculature that were observed in *LC3B*$^{-/-}$ mice were not replicated in *Beclin 1*$^{+/-}$ mice. We therefore conclude that the protection from the development of PH is more specifically dependent on the function of LC3B protein, and is insensitive to disruption of Beclin 1. We cannot exclude the possibility that phenotypic observations in *LC3B*$^{-/-}$ mice with respect to vascular function are caused by genomic instability resulting from impaired homoeostasis and increased metabolic stress in these animals. The testing of this hypothesis is beyond the scope of the current manuscript.

Because the HIF-1 represents a major regulator of the mammalian hypoxic response (42), and has recently been implicated in the regulation of autophagy (43), we therefore hypothesized that LC3B may regulate vascular proliferation through modulation of the HIF-1 signaling pathway. HIF-1 regulates several target genes in response to hypoxia, which have been proposed to play a role in cell proliferation and the pathogenesis of PH (i.e., endothelin-1, PDGF, angiotensin-converting enzyme, vascular endothelin growth factor, and so forth) (42). Recent studies implicate HIF-1 in the regulation of hypoxia-induced autophagy, through activation of the HIF1 target gene *bnip3* (43), although the role of this pathway has not been examined in PH. In our current studies, we show that LC3B knockdown alone increases the formation of intracellular ROS in vascular cells, and increases the stabilization of HIF-1α under both normoxic and hypoxic conditions. These results suggested that LC3B may act as an inhibitor of hypoxic signaling through the HIF-1α pathway. These observations may account for the enhanced vascular proliferation observed in LC3B knockdown cells.

Previous studies have described several additional alternative functions of LC3B in addition to its role in the autophagic pathway. LC3B acts as a positive regulator of fibronectin (*Fn1*) mRNA translation, through direct binding to an AU-rich region of the *Fn1 3′*-UTR (44, 45). LC3B-dependent fibronectin expression and downstream increases in connective tissue growth factor expression were associated with tumor cell proliferation, adhesion, and invasiveness in fibrosarcoma cells (46). Additionally, LC3B acts as a regulator of microtubule assembly (47) and microtubule-dependent mRNA transport (48). Although we did not examine these pathways, we cannot exclude the possibility that these mechanisms contribute to the phenotypic observations

in *LC3B*$^{-/-}$ mice. The testing of this hypothesis is beyond the scope of the current manuscript.

It should be noted that *LC3B*$^{-/-}$ mice display no impairment of basal autophagy or survival, and no neurodegenerative phenotype. Thus, LC3B function is likely compensated by other endogenous proteins, with respect to developmental and basal homeostatic processes (23). We cannot exclude the possibility that nonautophagic functions of LC3B, secondary to the activation of autophagy during hypoxia, are responsible for the vascular effects in this model.

The demonstration of altered autophagic flux in *in vivo* models, as it may relate to disease mechanism, represents a current challenge in the field. Advances in this area using the *in vivo* application of chemical inhibitors are currently the subject of intensive development in our laboratory, and in the laboratories of experts in the autophagy community. A recent review has identified this as a major challenge to the field and an important area requiring further development (25). In our current studies, the functional differences in the hypoxic response of the lung vasculature that were observed in *LC3B*$^{-/-}$ mice were not replicated in mice treated with the autophagic inhibitor chloroquine. Chloroquine injection also failed to modulate the vascular response to monocrotaline, an alternative model of PH generation, in rats (Figure E5). Chloroquine has been previously evaluated for use as an inhibitor of autophagic flux *in vivo* (49). The further implementation of inhibitors of autophagic flux *in vivo* in our model systems is an area of active development in our laboratory that will be the basis of future studies.

In addition to HIF-1, recent studies suggest that other major transcription factors, including C/EBPα and Egr-1, induced by hypoxia may also play a role in hypoxic vascular regulation (50). Egr-1 can regulate apoptotic, inflammatory, and coagulant cascades (51). We report here an essential role for Egr-1 in the regulation of hypoxia-induced autophagy *in vivo* and *in vivo.* Our studies show that Egr-1 plays a major role in the hypoxic activation of LC3B *in vitro*, primarily at a transcriptional level. Hypoxic activation of the autophagic process, as indicated by LC3B and LAMP1 co-localization, and total lung LC3B expression is greatly diminished in *Egr-1*$^{-/-}$ mice. We have observed aggravated indices of PH in animals genetically deleted for Egr-1 in the chronic hypoxia model. These results are consistent with a regulatory role for Egr-1 in LC3B expression.

Our recent studies have explored the role of caveolae in the regulation of membrane-dependent signaling processes (52). Caveolin-1, a resident protein of caveolae, regulates several signal transduction proteins, including G_i protein, Src family kinase, Ha-Ras, cyclooxygenase-2, and endothelial nitric oxide synthase (53–55). The importance of caveolin-1 in vascular processes has been demonstrated in studies of *cav-1*$^{-/-}$ mice, which display cardiac and lung abnormalities and PH (56–58). Chronic hypoxia treatment causes a delocalization of both caveolin-1 and endothelial nitric oxide synthase from the lipid raft leading to the cytoplasmic sequestration of these factors (59). We demonstrate the caveolae localization of autophagic protein LC3B and of transcription factor Egr-1, reported here to regulate *LC3B* transcription. The occurrence of these factors in caveolae and their associations with caveolin-1 under basal states imply a negative regulatory role of caveolin-1 in the activation of autophagy. Our observations that hypoxia mobilizes these factors from caveolae to cytoplasm in association with autophagic activation suggest that these translocations represent early events in hypoxic activation of autophagy. Our data indicate that the time-dependent dissociation of LC3B or Egr-1 from caveolin-1 can be detected in caveolae in response to hypoxia. These results suggest an upstream regulatory switch for activation of autophagy in vascular cells.

In conclusion, our identification of enhanced autophagic protein LC3B in clinical samples of human PH lung and lung vasculature, and in corresponding *in vivo* models of hypoxia-induced PH, warrants further investigation in the role of autophagic process in PH. Our results describe novel mechanisms for the activation of autophagic protein LC3B in response to noxious environmental stimuli, which include the release of this protein and its transcriptional regulators from a basal subcellular compartmentalization in plasma membrane caveolae. The identification of caveolin-1 and Egr-1 as novel regulators of autophagic protein LC3B suggests new targets for therapeutic manipulation of this homeostatic process.

Our functional experiments using *LC3B*$^{-/-}$ mice, and corresponding *in vitro* experiments in cultured vascular cells, demonstrate a specific antiproliferative and antihypertensive role for the autophagic protein LC3B in the development of hypoxia-induced PH. We conclude that these regulatory effects of LC3B depend on the modulation of the hypoxic proliferative response through the HIF-1α pathway.

Author Disclosure: S-J.L. is employed by Brigham and Women's Hospital as an academic appointment. A.S. is employed by Brigham and Women's Hospital as a research fellow. L.G. does not have a financial relationship with a commercial entity that has an interest in the subject of this manuscript. T-P.A. does not have a financial relationship with a commercial entity that has an interest in the subject of this manuscript. M.L. does not have a financial relationship with a commercial entity that has an interest in the subject of this manuscript. H.S. received $10,001–$50,000 from the Oak Foundation in sponsored grants. X.L. is employed by Brigham and Women's Hospital as an academic appointment. Z-H.C. does not have a financial relationship with a commercial entity that has an interest in the subject of this manuscript. E.I. is employed by Brigham and Women's Hospital as a laboratory manager. Y.J. does not have a financial relationship with a commercial entity that has an interest in the subject of this manuscript. C.F-B. does not have a financial relationship with a commercial entity that has an interest in the subject of this manuscript. S.W.R. is employed by Brigham and Women's Hospital as a regular academic appointment, received $10,001–$50,000 from the NIH in sponsored grants as co-investigatorships, and received salary support from the Lovelace Respiratory Research Institute. H.P.K. is employed by the University of Ulsan as an Assistant Professor. M.R. received up to $1,000 from the NIH/NHLBI for serving on an advisory board. A.M.K.C. does not have a financial relationship with a commercial entity that has an interest in the subject of this manuscript.

Acknowledgment: The authors thank N. Mizushima for the green fluorescence protein-LC3 construct and B. Levine for the *Beclin 1*$^{+/-}$ mice.

References

1. Rabinovitch M. Molecular pathogenesis of pulmonary arterial hypertension. *J Clin Invest* 2008;118:2372–2379.
2. Simonneau G, Robbins IM, Beghetti M, Channick RN, Delcroix M, Denton CP, Elliott CG, Gaine SP, Gladwin MT, Jing ZC, *et al.* Updated clinical classification of pulmonary hypertension. *J Am Coll Cardiol* 2009;54:S43–S54.
3. Farber HW, Loscalzo J. Pulmonary arterial hypertension. *N Engl J Med* 2004;351:1655–1665.
4. Tuder RM, Abman SH, Braun T, Capron F, Stevens T, Thistlethwaite PA, Haworth SG. Development and pathology of pulmonary hypertension. *J Am Coll Cardiol* 2009;54:S3–S9.
5. Chan SY, Loscalzo J. Pathogenic mechanisms of pulmonary arterial hypertension. *J Mol Cell Cardiol* 2008;44:14–30.
6. Morrell NW, Adnot S, Archer SL, Dupuis J, Jones PL, MacLean MR, McMurtry IF, Stenmark KR, Thistlethwaite PA, Weissmann N, *et al.* Cellular and molecular basis of pulmonary arterial hypertension. *J Am Coll Cardiol* 2009;54:S20–S31.
7. Giaid A, Saleh D. Reduced expression of endothelial nitric oxide synthase in the lungs of patients with pulmonary hypertension. *N Engl J Med* 1995;333:214–221.
8. Stewart DJ, Levy RD, Cernacek P, Langleben D. Increased plasma endothelin-1 in pulmonary hypertension: marker or mediator of disease? *Ann Intern Med* 1991;114:464–469.
9. Mandegar M, Yuan JX. Role of K^+ channels in pulmonary hypertension. *Vascul Pharmacol* 2002;38:25–33.
10. Stenmark KR, Fagan KA, Frid MG. Hypoxia-induced pulmonary vascular remodeling. Cellular and molecular mechanisms. *Circ Res* 2006;99:675–691.
11. Masri FA, Xu W, Comhair SA, Asosingh K, Koo M, Vasanji A, Drazba J, Anand-Apte B, Erzurum SC. Hyperproliferative apoptosis-resistant endothelial cells in idiopathic pulmonary arterial hypertension. *Am J Physiol Lung Cell Mol Physiol* 2007;293:L548–L554.

12. Mizushima N, Levine B, Cuervo AM, Klionsky DJ. Autophagy fights disease through cellular self-digestion. *Nature* 2008;451:1069–1075.
13. Levine B, Klionsky DJ. Development by self-digestion: molecular mechanisms and biological functions of autophagy. *Dev Cell* 2004;6:463–477.
14. Martinet W, De Meyer GR. Autophagy in atherosclerosis: a cell survival and death phenomenon with therapeutic potential. *Circ Res* 2009;104:304–317.
15. De Meyer GR, Martinet W. Autophagy in the cardiovascular system. *Biochim Biophys Acta* 2009;1793:1485–1495.
16. Yorimitsu T, Klionsky DJ. Autophagy: molecular machinery for self-eating. *Cell Death Differ* 2005;12:1542–1552.
17. Bampton ET, Goemans CG, Niranjan D, Mizushima N, Tolkovsky AM. The dynamics of autophagy visualized in live cells: from autophagosome formation to fusion with endo/lysosomes. *Autophagy* 2006;1:23–36.
18. Tanida I, Minematsu-Ikeguchi N, Ueno T, Kominami E. Lysosomal turnover, but not a cellular level, of endogenous LC3 is a marker for autophagy. *Autophagy* 2005;1:84–91.
19. Levine B, Kroemer G. Autophagy in the pathogenesis of disease. *Cell* 2008;132:27–42.
20. Lee SJ, Kim HP, Choi AMK. Autophagy represents an adaptive stress response to offset the development of pulmonary arterial hypertension [abstract]. *Am J Respir Crit Care Med* 2009;179:A1813.
21. Lee SJ, Kim HP, Choi AMK. Egr-1-dependent autophagy inhibits the development of pulmonary arterial hypertension [abstract]. *Am J Respir Crit Care Med* 2009;179:A1814.
22. Eskelinen E-L. Fine structure of the autophagosome. *Methods Mol Biol* 2008;445:11–28.
23. Cann GM, Guignabert C, Ying L, Deshpande N, Bekker JM, Wang L, Zhou B, Rabinovitch M. Developmental expression of LC3alpha and beta: absence of fibronectin or autophagy phenotype in LC3beta knockout mice. *Dev Dyn* 2008;237:187–195.
24. Qu X, Yu J, Bhagat G, Furuya N, Hibshoosh H, Troxel A, Rosen J, Eskelinen EL, Mizushima N, Ohsumi Y, *et al.* Promotion of tumorigenesis by heterozygous disruption of the beclin 1 autophagy gene. *J Clin Invest* 2003;112:1809–1820.
25. Mizushima N, Yoshimori T, Levine B. Methods in mammalian autophagy research. *Cell* 2010;140:313–326.
26. Kabeya Y, Mizushima N, Ueno T, Yamamoto A, Kirisako T, Noda T, Kominami E, Ohsumi Y, Yoshimori T. LC3, a mammalian homologue of yeast Apg8p, is localized in autophagosome membranes after processing. *EMBO J* 2000;19:5720–5728.
27. Chandel NS, McClintock DS, Feliciano CE, Wood TM, Melendez JA, Rodriguez AM, Schumacker PT. Reactive oxygen species generated at mitochondrial complex III stabilize hypoxia-inducible factor-1alpha during hypoxia: a mechanism of O_2 sensing. *J Biol Chem* 2000;275:25130–25138.
28. Chen ZH, Kim HP, Sciurba FC, Lee SJ, Feghali-Bostwick C, Stolz DB, Dhir R, Landreneau RJ, Schuchert MJ, Yousem SA, *et al.* Egr-1 regulates autophagy in cigarette smoke-induced chronic obstructive pulmonary disease. *PLoS ONE* 2008;3:e3316.
29. Cohen AW, Hnasko R, Schubert W, Lisanti MP. Role of caveolae and caveolins in health and disease. *Physiol Rev* 2004;84:1341–1379.
30. Levine B. Cell biology: autophagy and cancer. *Nature* 2007;446:745–747.
31. Kondo Y, Kanzawa T, Sawaya R, Kondo S. The role of autophagy in cancer development and response to therapy. *Nat Rev Cancer* 2005;5:726–734.
32. Boland B, Kumar A, Lee S, Platt FM, Wegiel J, Yu WH, Nixon RA. Autophagy induction and autophagosome clearance in neurons: relationship to autophagic pathology in Alzheimer's disease. *J Neurosci* 2008;28:6926–6937.
33. Rioux JD, Xavier RJ, Taylor KD, Silverberg MS, Goyette P, Huett A, Green T, Kuballa P, Barmada MM, Datta LW, *et al.* Genome-wide association study identifies new susceptibility loci for Crohn disease and implicates autophagy in disease pathogenesis. *Nat Genet* 2007;39:596–604.
34. Galluzzi L, Vicencio JM, Kepp O, Tasdemir E, Maiuri MC, Kroemer G. To die or not to die: that is the autophagic question. *Curr Mol Med* 2008;8:78–91.
35. Kroemer G, Levine B. Autophagic cell death: the story of a misnomer. *Nat Rev Mol Cell Biol* 2008;9:1004–1010.
36. Steiner MK, Syrkina OL, Kolliputi N, Mark EJ, Hales CA, Waxman AB. Interleukin-6 overexpression induces pulmonary hypertension. *Circ Res* 2009;104:236–244.
37. Said SI, Hamidi SA, Dickman KG, Szema AM, Lyubsky S, Lin RZ, Jiang YP, Chen JJ, Waschek JA, Kort S. Moderate pulmonary arterial hypertension in male mice lacking the vasoactive intestinal peptide gene. *Circulation* 2007;115:1260–1268.
38. Nakai A, Yamaguchi O, Takeda T, Higuchi Y, Hikoso S, Taniike M, Omiya S, Mizote I, Matsumura Y, Asahi M, *et al.* The role of autophagy in cardiomyocytes in the basal state and in response to hemodynamic stress. *Nat Med* 2007;13:619–624.
39. Kuma A, Hatano M, Matsui M, Yamamoto A, Nakaya H, Yoshimori T, Ohsumi Y, Tokuhisa T, Mizushima N. The role of autophagy during the early neonatal starvation period. *Nature* 2004;432:1032–1036.
40. Matsui Y, Takagi H, Qu X, Abdellatif M, Sakoda H, Asano T, Levine B, Sadoshima J. Distinct roles of autophagy in the heart during ischemia and reperfusion: roles of AMP-activated protein kinase and Beclin 1 in mediating autophagy. *Circ Res* 2007;100:914–922.
41. Karantza-Wadsworth V, Patel S, Kravchuk O, Chen G, Mathew R, Jin S, White E. Autophagy mitigates metabolic stress and genome damage in mammary tumorigenesis. *Genes Dev* 2007;21:1621–1635.
42. Yildiz P. Molecular mechanisms of pulmonary hypertension. *Clin Chim Acta* 2009;403:9–16.
43. Zhang H, Bosch-Marce M, Shimoda LA, Tan YS, Baek JH, Wesley JB, Gonzalez FJ, Semenza GL. Mitochondrial autophagy is an HIF-1-dependent adaptive metabolic response to hypoxia. *J Biol Chem* 2008;283:10892–10903.
44. Zhou B, Boudreau N, Coulber C, Hammarback J, Rabinovitch M. Microtubule-associated protein 1 light chain 3 is a fibronectin mRNA-binding protein linked to mRNA translation in lamb vascular smooth muscle cells. *J Clin Invest* 1997;100:3070–3082.
45. Zhou B, Rabinovitch M. Microtubule involvement in translational regulation of fibronectin expression by light chain 3 of microtubule-associated protein 1 in vascular smooth muscle cells. *Circ Res* 1998;83:481–489.
46. Ying L, Lau A, Alvira CM, West R, Cann GM, Zhou B, Kinnear C, Jan E, Sarnow P, Van de Rijn M, *et al.* LC3-mediated fibronectin mRNA translation induces fibrosarcoma growth by increasing connective tissue growth factor. *J Cell Sci* 2009;122:1441–1451.
47. Mann SS, Hammarback JA. Molecular characterization of light chain 3. A microtubule binding subunit of MAP1A and MAP1B. *J Biol Chem* 1994;269:11492–11497.
48. Seidenbecher CI, Landwehr M, Smalla KH, Kreutz M, Dieterich DC, Zuschratter W, Reissner C, Hammarback JA, Böckers TM, Gundelfinger ED, *et al.* Caldendrin but not calmodulin binds to light chain 3 of MAP1A/B: an association with the microtubule cytoskeleton highlighting exclusive binding partners for neuronal Ca^{2+}-sensor proteins. *J Mol Biol* 2004;336:957–970.
49. Iwai-Kanai E, Yuan H, Huang C, Sayen MR, Perry-Garza CN, Kim L, Gottlieb RA. A method to measure cardiac autophagic flux in vivo. *Autophagy* 2008;4:322–329.
50. Liao H, Hyman MC, Lawrence DA, Pinsky DJ. Molecular regulation of the PAI-1 gene by hypoxia: contributions of Egr-1, HIF-1α, and C/EBPα. *FASEB J* 2007;21:935–949.
51. Liu C, Calogero A, Ragona G, Adamson E, Mercola D. EGR-1, the reluctant suppression factor: EGR-1 is known to function in the regulation of growth, differentiation, and also has significant tumor suppressor activity and a mechanism involving the induction of TGF-β1 is postulated to account for this suppressor activity. *Crit Rev Oncog* 1996;7:101–125.
52. Nakahira K, Kim HP, Geng XH, Nakao A, Wang X, Murase N, Drain PF, Wang X, Sasidhar M, Nabel EG, *et al.* Carbon monoxide differentially inhibits TLRs signaling pathways by regulating ROS-induced trafficking of TLRs to lipid rafts. *J Exp Med* 2006;203:2377–2389.
53. Li S, Okamoto T, Chun M, Sargiacomo M, Casanova JE, Hansen SH, Nishimoto I, Lisanti MP. Evidence for a regulated interaction between heterotrimeric G proteins and caveolin. *J Biol Chem* 1995;270:15693–15701.
54. Schlegel A, Lisanti MP. The caveolin triad: caveolae biogenesis, cholesterol trafficking, and signal transduction. *Cytokine Growth Factor Rev* 2001;12:41–51.
55. Liou JY, Deng WG, Gilroy DW, Shyue SK, Wu KK. Colocalization and interaction of cyclooxygenase-2 with caveolin-1 in human fibroblasts. *J Biol Chem* 2001;276:34975–34982.
56. Drab M, Verkade P, Elger M, Kasper M, Lohn M, Lauterbach B, Menne J, Lindschau C, Mende F, Luft FC, *et al.* Loss of caveolae, vascular dysfunction, and pulmonary defects in caveolin-1 gene-disrupted mice. *Science* 2001;293:2449–2452.
57. Razani B, Engelman JA, Wang XB, Schubert W, Zhang XL, Marks CB, Macaluso F, Russell RG, Li M, Pestell RG, *et al.* Caveolin-1 null mice are viable but show evidence of hyperproliferative and vascular abnormalities. *J Biol Chem* 2001;276:38121–38138.
58. Zhao YY, Liu Y, Stan RV, Fan L, Gu Y, Dalton N, Chu PH, Peterson K, Ross J, Chien KR. Defects in caveolin-1 cause dilated cardiomyopathy and pulmonary hypertension in knockout mice. *Proc Natl Acad Sci USA* 2002;99:11375–11380.
59. Mukhopadhyay S, Xu F, Sehgal PB. Aberrant cytoplasmic sequestration of eNOS in endothelial cells after monocrotaline, hypoxia, and senescence: live-cell caveolar and cytoplasmic NO imaging. *Am J Physiol Heart Circ Physiol* 2007;292:H1373–H1389.